Reaction Chemistry & Engineering

ROYAL SOCIETY OF CHEMISTRY

PAPER

View Article Online
View Journal | View Issue

Check for updates

Cite this: *React. Chem. Eng.*, 2024, **9**, 2623

Lipase-catalysed esterification in a reactive natural deep eutectic solvent leads to lauroylcholine chloride rather than glucose ester†

Alina Ramona Buzatu, [ab] Miguel Angel Soler, *[c] Ozge Ozkilinc, [c] Sara Fortuna, ‡[d] Diana Maria Dreavă, [a] Ioan Bîtcan,[a] Paolo Giannozzi, [ce] Federico Fogolari, [c] Lucia Gardossi, [f] Francisc Peter, [a] Anamaria Todea[a] and Carmen Gabriela Boeriu *[a]

Received 19th April 2024,
Accepted 4th July 2024

DOI: 10.1039/d4re00209a

rsc.li/reaction-engineering

Enzymatic esterification of glucose with lauric acid catalyzed by lipase B from *Candida antarctica* immobilized on acrylic resin (LAR) was investigated in hydrophilic reactive natural deep eutectic solvents (R-NADESs), composed of choline chloride (ChCl) as the hydrogen bond acceptor (HBA) and glucose (Glc) and water as hydrogen bond donors (HBDs) in different molar ratios. Surprisingly, no glucose esters were obtained, the only esterification product being lauroylcholine chloride, obtained in the ChCl : Glc : H_2O (2 : 1 : 1) ternary R-NADES. Molecular dynamic simulations clearly explained this unexpected selectivity, showing that the lipase-catalyzed synthesis of glucose lauryl esters is hindered by the manifold and strong interactions in the H-bond network and the formation of voluminous adducts of glucose with the chloride ion, which cannot access the alcohol catalytic subsite. The free choline chloride, not involved in the H-bond network of the ChCl : Glc : H_2O (2 : 1 : 1) R-NADES, did enter the CalB catalytic pocket and was converted to the corresponding lauroylcholine ester.

Introduction

Glucose fatty acid esters belong to the larger group of sugar derived fatty acid esters (SFAEs), an essential collection of biobased surfactants with application as emulsifiers in food and personal care products, drug delivery systems, solubilizing agents, or lubricants.[1] Composed entirely of biobased materials, *i.e.*, carbohydrates from common biorefinery feedstocks and fatty acids from oilseeds or from oleochemical coproducts, SFAEs are intrinsically natural. However, current synthetic chemo-catalytic processes, although efficient, are energy-intensive, non-selective and use volatile organic solvents, and therefore only partially fulfill green process requirements.

One of the best approaches to overcome the current limitations of SFAE production is the integration of regioselective biocatalysis with green solvents, of which the most promising are deep eutectic solvents (DESs) and their greenest counterparts, the natural deep eutectic solvents (NADESs).[2,3] DES and NADES systems are complex hydrogen-bond networks formed by a hydrogen bond acceptor (HBA), usually a quaternary ammonium salt, and hydrogen bond donors (HBDs), like alcohols, amides, carboxylic acids, carbohydrates, or polyols. Since they are non-volatile, nontoxic, biodegradable, and biocompatible, (NA)DESs are considered the best alternative to organic solvents and ionic liquids for greening chemical industrial processes.

Building up on the well documented use of microbial lipases for the synthesis of SFAEs[4–7] and increasing knowledge on the properties and applications of NADESs,[8–10] numerous studies were dedicated to the investigation of the synergy between enzymes and NADESs and their application for glycolipid synthesis. The remarkable finding that lipases preserve their secondary structure,[11] thermal stability,[12] and catalytic activity[13] in both hydrophobic and hydrophilic (NA)DESs was a major step forward.

[a] *Faculty of Industrial Chemistry and Environmental Engineering, University Politehnica Timisoara, Carol Telbisz 6, 300001 Timisoara, Romania. E-mail: carmengabriela.boeriu@upt.ro*
[b] *Department of Biochemistry and Pharmacology, "Victor Babes" University of Medicine and Pharmacy, Eftimie Murgu Sq. No. 2, 300041 Timisoara, Romania*
[c] *Dipartimento di Scienze Matematiche, Informatiche e Fisiche, Università di Udine, Via delle Scienze 206, 33100 Udine, Italy. E-mail: miguelangel.solerbastida@uniud.it*
[d] *Dipartimento di Scienze Chimiche e Farmaceutiche, Università degli Studi di Trieste, Piazzale Europa 1, Trieste, 34127, Italy*
[e] *CNR-IOM, Istituto dell'Officina dei Materiali, SISSA, I-34136 Trieste, Italy*
[f] *Dipartimento di Scienze Chimiche e Farmaceutiche, Università degli Studi di Trieste, Piazzale Europa 1, Trieste, 34127, Italy*
† Electronic supplementary information (ESI) available. See DOI: https://doi.org/10.1039/d4re00209a
‡ Currently at: Cresset – New Cambridge House, Bassingbourn Road, Litlington, Cambridgeshire, SG8 0SS, UK.

Several research groups reported on the lipase-catalysed synthesis of glucose esters by esterification and transesterification reactions in both hydrophilic and hydrophobic NADESs. Screening for the most suited NADES for the synthesis of glucose esters by transesterification with vinyl hexanoate catalysed by immobilized lipase B from *Candida antarctica* (N435), Pöhnlein *et al.*[14] found glucose-6-hexanoate only in ChCl : urea (1 : 2) and ChCl : Glc (1 : 1) NADES mixtures, but not in the ChCl : ethylene glycol (1 : 1) and (1 : 2) and the ChCl : glycerol (1 : 1) eutectics. However, authors found tiny amounts of choline chloride hexanoate in all evaluated NADESs. Besides, the formation of 4,6-dimethylidene glucose was observed in a secondary reaction between glucose and the acetaldehyde by-product.[14] Similarly, glucose-6-decanoate was synthesised by transesterification with vinyl decanoate in a ChCl : urea (1 : 2) NADES,[15] in a hydrophilic ChCl : Glc : H_2O (5 : 1 : 5) NADES,[13] and in a hydrophobic DES consisting of D-menthol and decanoic acid.[16]

Siebenhaller *et al.*,[17] reported the synthesis of monoesters, *i.e.*, glucose-6-octanoate and diesters, like glucose dipalmitate, dioleate, and dilinoleate, by transesterification with the corresponding methyl and vinyl esters of the C6–C18 fatty acids, catalysed by N435 in a reactive NADES obtained from beechwood cellulose fibre hydrolysate and ChCl. They also observed the formation of secondary products, such as levoglucosan, by condensation of glucose with the acetaldehyde generated by tautomerisation of the vinyl alcohol by-product. The same research group stated that water addition was essential for the lipase catalysed synthesis of arabinose laurate esters in a ChCl : arabinose NADES, the yields increasing at 4% water content in the NADES.[17]

Adding up to the current state of the art research that is focusing on enzymatic transesterification of glucose in NADES mixtures, we directed our studies to the investigation of the enzymatic glucose esterification with free fatty acids in hydrophilic reactive NADES systems. Although transesterification is efficient and relatively high ester yields can be obtained, it shows several drawbacks and limitations:

(i) hydrolysis of the methyl or vinyl ester reagents with the formation of free fatty acids and water, even in eutectics with low water content, due to hygroscopicity of choline chloride; hydrolysis is preferred by lipase over transesterification. Indeed Semproli *et al.*[15] showed that hydrolysis of vinyl esters is the preferred pathway for lipase when the target substrate is unfavoured.

(ii) Formation of secondary products in condensation reactions with the acetaldehyde formed from tautomerisation of the vinyl alcohol released in the transesterification reaction and/or in reactions of the vinyl ester with NADES constituents like polyols (*i.e.*, ethylene glycol, glycerol) and urea.

(iii) Deactivation of the enzyme, due to Schiff-base formation by condensation of acetaldehyde with the free amine groups of surface lysine residues.

(iv) Complex downstream processing due to a multi-component composition of the product mixture with different physical properties.

Esterification reactions instead, are greener, using only bio-based and natural reagents and efficient under optimal conditions. Recently, we proved the enzymatic synthesis of α,ω-lauryl diesters of carbohydrate polyols, with good yields and excellent regioselectivity by esterification in a ChCl–polyol R-NADES with a dual function, acting as a solvent and substrate source.[18] Thus, this study focused on the investigation of hydrophilic R-NADES mixtures for the enzymatic synthesis of glucose lauryl esters by esterification. We prepared and characterised two novel ternary R-NADESs containing ChCl, glucose and water in different molar ratios, and we investigated in detail the influence of the R-NADES composition and properties on the esterification activity and operational stability of the biocatalyst. Computational simulations gave a clear and comprehensive view of the H-bond network, and the interactions between the components and their mobility. Optimization of the reaction conditions allowed preparative synthetic reactions. Surprisingly, the product of the reaction was identified as choline chloride lauryl ester, a bio-based ester that might be a valuable biosurfactant. Glucose monolaurate was not obtained. Molecular modelling and simulations fully explained the experimental results and helped to rationalise all the interactions and effects governing the complex reaction system. This work brings together new insights in the complex behaviour of NADESs and R-NADESs, showing that natural eutectic mixtures are unique systems that cannot be generalised, and must be designed for each case and reaction. A multidisciplinary approach, including computational modelling, reaction engineering, solvent engineering and experimental research should be integrated. Scheme 1 illustrates the possible pathways for lipase-catalysed esterification of a reactive NADES containing choline chloride and glucose as major components.

Experimental

Materials

Choline chloride (≥98%) and lipase B from *Candida antarctica*, recombinant, expressed in *Aspergillus niger*, immobilized on acrylic resin (LAR), with a specific activity ≥5000 U g^{-1} (propyl laurate hydrolysis), were obtained from Sigma-Aldrich. Dimethyl sulfoxide (DMSO), hexane and tetrahydrofuran (THF) were obtained from Merck. Lauric acid (LA), 98% was obtained from Alfa Aesar. Ethanol was obtained from Chimopar (Bucharest, Romania). Anhydrous D-(+)-glucose was obtained from Fluka. Ethyl acetate was obtained from Chimreactiv (Bucharest, Romania). Alumina silica gel plates (DC-Autofolien Kiesegel 60 F254) were obtained from Merck, Kenilworth, NJ, USA.

Preparation and characterisation of R-NADES

Ternary R-NADESs, consisting of choline chloride (ChCl), anhydrous D-(+)-glucose (Glc) and water at 1 : 1 : 1 and 2 : 1 : 1 molar ratios, were prepared and characterized as previously described for carbohydrate polyol-based R-NADESs.[18]

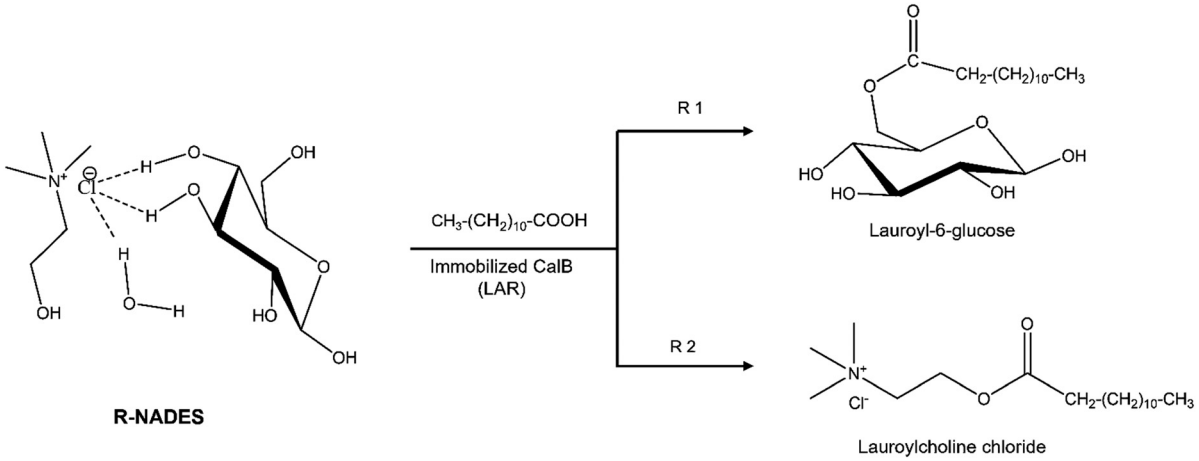

Scheme 1 Possible pathways for lipase-catalysed esterification of a reactive NADES containing choline chloride, glucose and water, obtaining lauroyl-6-glucose (R1) and/or lauroylcholine chloride.

Thermal properties and dynamic viscosity were measured by thermogravimetry (TG), differential scanning calorimetry (DSC) and rheology.

Biocatalyst characterisation

Catalytic activity. The esterification activity of LAR was determined for the synthesis of *n*-propyl laurate in (a) a solvent-free system, as reference, and (b) in ternary R-NADESs, using the initial rate methodology.[18] One activity unit (U) is the amount of propyl laurate (μmol) produced per minute by one gram of enzyme. Values reported are a mean of three experiments.

The esterification activity in the solvent free system was determined in an equimolar reaction mixture consisting of 2 mmol of LA and 2 mmol of *n*-propanol. The reactions were initiated by addition of 10 mg LAR, were carried out at 55 °C in 2 ml capped vials, and stirred at 350 rpm in a thermomixer (Thermomixer comfort, Eppendorf, Germany) for 1 hour. Aliquots of 0.1 ml were withdrawn at regular time intervals and mixed with 7 ml ethanol, followed by titration with ethanolic KOH 0.1 M solution, with phenolphthalein as endpoint indicator, to determine the unreacted LA. The amount of propyl laurate (μmol) yielded at different times during the linear phase of the reaction was calculated from the determined converted LA, according to the (1 : 1) stoichiometry of the reaction.

The esterification activity of LAR in the R-NADES systems was determined with the initial rate method used for the reference activity described for the solvent free system, with some differences that are detailed below. The reaction mixture consisted of 0.4 mmol of LA, 0.4 mmol of 1-propanol and 0.8 g R-NADES at 70 °C, and 50 reference units LAR. The mixture was stirred at 70 °C and 1000 rpm for 4 hours. Aliquot samples were accurately weighed to determine their mass, prior to dissolution in ethanol and titration.

Stability. The stability of LAR in ternary R-NADES mixtures was determined upon incubation of the lipase in the R-NADES at 70 °C for 0, 24, 48 and 72 hours, followed by addition of LA and 1-propanol and determination of the esterification activity. The stability of lipase is given as relative activity (%), as previously described.[18]

General procedure for lipase catalysed esterification of the R-NADES with LA

In a 5 mL Eppendorf tube, LA was mixed with the R-NADES at a 1 : 1 molar ratio of LA to glucose. The reaction was started by the addition of the LAR biocatalyst, in amounts ranging from 285 to 1600 U g^{-1} glucose (reference esterification activity, for *n*-propyl laurate synthesis). The reaction mixture was incubated for 24 to 72 hours, at: a) 60 °C, at 30 rpm in a Benchmark Rhoto-Term™ incubated tubes rotator (Benchmark Scientific, Sayreville, NJ, USA), and b) 70 °C and 75 °C in a thermomixer, at 600 rpm. Reaction products were extracted by sequential addition of organic solvents (THF, hexane, ethyl acetate and ethanol). Three control reactions were conducted under similar reaction conditions, but removing one component at a time, as follows: (i) without enzyme, (ii) without NADES and (iii) without LA. Reaction mixtures and controls were analysed by HPLC. The concentration of LA in the samples was determined from the LA calibration curve built up by HPLC analysis. LA conversion (mol%) was determined based on the moles of LA in the control without enzyme and in the sample. No conversion of lauric acid was observed for control reactions. All reactions, including controls, were performed in duplicate, and the results given are an average of two experiments. At the end of the reaction, the reaction mixture was extracted with THF, at 40 °C, for 30 minutes. HPLC and TLC analysis of the extract showed the lauric acid peak (R_t = 7.70 min, R_f = 0.27) and a product peak (R_t = 9.54 min, R_f = 0.73). After concentration by evaporation, the mixture was separated by silica gel chromatography, with ethyl acetate/hexane (1 : 9) as eluent. The fractions collected were analysed by TLC, and the fractions showing the spot at R_f = 0.73 were

pooled together and evaporated to dryness by vacuum evaporation. The product obtained was identified as lauroylcholine chloride by FTIR, 1H-NMR, and 13C-NMR spectroscopy.

Identification and characterisation of reaction products

After the reaction, samples were analysed by (a) thin layer chromatography (TLC) and (b) high performance liquid chromatography (HPLC). TLC was carried out on alumina silica gel plates (Merck, Kenilworth, NJ, USA, DC-Autofolien Kiesegel 60 F254) with dimensions 20 × 20 cm and 0.2 mm thick. The mobile phase was a mixture of ethyl acetate : hexane (1 : 9). Visualization of the spots was performed by immersing the plate in an ethanolic solution of phosphomolybdic acid with a 5% concentration, followed by heating. The R_f values for LA and lauroylcholine chloride were: R_f LA = 0.27 and R_f lauroylcholine chloride = 0.73. HPLC analysis was performed using an Agilent system HPLC 1260 INFINITY II chromatograph equipped with a Luna 5 μm phenyl-hexyl LC column 250 × 4.6 mm, 100 Å, (Phenomenex, USA), a quaternary G7111B pump, a column thermostat (Agilent Technology Germany), a RID WR G7162A detector, and OpenLab CDS Workstation software. The samples were eluted using a methanol/water 90 : 10 mixture, at a 0.5 mL min^{-1} flow rate and 40 °C. LA conversions (mol%) were calculated based on the calibration curve of LA.

Esters were purified by silica gel column chromatography, with ethyl acetate/hexane (1 : 9) eluent. Products were identified by FTIR and NMR spectroscopy. FTIR spectra were acquired in attenuated total reflectance mode (ATR) on a Bruker Vertex 70 spectrometer (Bruker Daltonik GmbH, Bremen, Germany). ^{1}H-NMR spectra were recorded on a Bruker Avance III spectrometer (400.17 MHz) and internally referenced to the residual solvent signal ($CDCl_3$: δ 7.26 ppm, D_2O: δ 4.79). ^{13}C-NMR spectra were recorded on a Bruker Avance III (100.62 MHz) and internally referenced to the residual solvent signal ($CDCl_3$: δ 77 ppm). All NMR spectra were measured at 298 K.

Computational simulations

Modelling of lauric acid, R-NADESs and CalB lipase. R-NADESs with choline chloride (ChCl) salt, α- and β-D-glucose and water mixtures in proportions 2 : 0.5 : 0.5 : 1 and 1 : 0.5 : 0.5 : 1 respectively were constructed using the program Packmol.[19] The structure of lipase B from *Candida antarctica* (CalB) was available in the Protein Data Bank (PDB ID: 1TCA).[20] All CalB + R-NADES + lauric acid (LA) systems were constructed by placing the protein at the centre of the box and then filling the box with the R-NADES mixture according to the experimental molar ratios, *i.e.*, ChCl : glucose : water : LA of 2 : 1 : 1 : 1 and 1 : 1 : 1 : 1, respectively. The number of molecules in each constructed cubic box mixture is described in Table S1.† The structures of the R-NADES components and lauric acid were obtained from the CHARMM Small Molecule Library from CHARMM-GUI.[21] Overall, three different systems were prepared for each R-NADES mixture: (i) a simulation box of the R-NADES; (ii) R-NADES + CalB, and (iii) R-NADES + CalB + LA.

Molecular dynamics simulations. Prior to performing molecular dynamics (MD) simulations, a minimization of the systems that contain the protein CalB were performed in two steps: (a) first the protein was restrained, and the solvent energy was minimized for 10 000 steps and with an initial energy minimization step size of 0.001 nm, and (b) second, an unrestrained minimization was performed using the same minimization parameters. For the systems containing only the R-NADES, the minimization is reduced to the second step of the previous minimization protocol. After minimization, a set of molecular dynamics simulations mimicking the same experimental conditions (343, 15 K (70 °C) and 1 bar) was performed. The computational protocol employed in this work is based on the one developed in our previous work.[18] In summary, the solvent system was relaxed for 1 ns at 343.15 K and at constant pressure (1 bar) while the protein structure was restrained, checking that no further changes were observed in the density of the systems. To accelerate the mixing of the R-NADES components, we subsequently followed a simulated annealing scheme.[18] Thus, the temperature was linearly increased to 500 K during 100 ns and remained at 500 K for a duration of 200 ns. We performed a sampling of configurations every 25 ns during the last 100 ns, obtaining 4 different snapshots for each system. All poses were subsequently cooled down to 343.15 K during 100 ns following the exponential function $T = 156.85 \times \exp(-0.05 \times t) + 343.15$. The parameters of the function were chosen manually to guarantee an initial fast rate cooling during the first 20 ns (achieving 400 K), following a much slower cooling until the end of the simulation. During all the simulated annealing processes, the backbone structure of the protein was restrained. Then, we employed each configuration at the end of the 4 cooling simulations to run 4 MD replicas at 343.15 K of each system with the protein structure unrestrained. The time length of R-NADES simulations (without protein) was 20 ns, while for the simulations including CalB, it was 100 ns. In the case of the system NADES + CalB + LA (2 : 1 : 1 : 1), the length of all 4 simulations was extended to 500 ns to assess the possible entrance of choline in the catalytic pocket.

All MD simulations were performed with the software package GROMACS v.2022,[22] and Charmm36 (ref. 23) and CGenFF 4.6 (ref. 24 and 25) force fields were employed for the parameterization of the system. Following ref. 26, the charges of choline and chloride atoms were scaled by a factor of 0.9, to intrinsically represent charge transfer in the nonpolarizable force field. The Verlet integrator and LINCS[27] constraints were employed with a time step of 1 fs for the equilibration process and 2 fs for the production phase. The temperature was controlled utilizing a modified Berendsen thermostat,[27] while an isotropic pressure of 1 bar was kept using a Parrinello–Rahman barostat,[28,29] with a time constant of 5 ps and an isothermal compressibility of 5×10^{-5} bar^{-1}.

Long-range electrostatic interactions were described by the smooth particle-mesh Ewald (PME) method by using a PME order of 4. Lennard-Jones (LJ) and electrostatic interactions were calculated with a cut-off radius of 1.2 nm, while LJ interactions were smoothly switched off between 1.0 and 1.2 nm.

Analysis of MD trajectories. Residue–residue interactions were first assessed through contact frequency analysis. A contact between two atoms is defined when their van der Waals surfaces are within a 0.5 Å distance. The cut-off chosen here is different from the most effective one (1 Å) tested on amino acids contacts,[30] because at first contacts were analysed at an atom–atom level. Only minor changes are observed on residue–residue contact frequencies between the two cut-off choices. For each snapshot, all the contacts between atoms not belonging to the same residue are listed. Then for each residue type (*i.e.* water, choline, chloride, α- and β glucose) the contacts involving each of their atoms are counted. The counts obtained in this way are used to obtain frequencies of occurrence of each atom of each residue in any contact, and the frequencies of each specific pairwise contact, by dividing them by the total number of contacts in the system. Atom–atom contacts are then used to compute the frequencies of each residue–residue contact.

The number of residue–residue contacts is the sum of all atom–atom contacts involving the pair of residues.

If we index each residue type by i and j and indicate by f_i and f_j the single contact frequencies of the residues i and j, and by f_{ij} the pairwise frequencies in the contacts, the ratio:

$$g_{ij} = f_{ij}/(f_i \times f_j) \quad (1)$$

provides an assessment of how much more (or less) frequent is a contact than expected by chance. This analysis has been performed both at the atom and residue levels, and pooling or not α- and β-glucose.

The number of hydrogen bonds (H-bonds) between the components of R-NADES was evaluated along the MD trajectories with the program *hbond* of GROMACS[22] by using the program standard distance and angle cut-off parameters of 3.5 Å and 30°, respectively. The type atoms of chloride ions were modified to oxygen in the GROMACS topology before performing the analysis, since the program only evaluates N and O atom types as H-bond donors and acceptors. For simplicity, the same H-bond cut-off was kept for chloride, although a slightly larger cutoff (3.8 A) has been used in the literature.[31]

Other structural analyses of the MD trajectories were conducted using the VMD software package.[32]

Results and discussion

R-NADES and their properties

Physical and thermal properties. Mixing choline chloride with glucose and water in different molar ratios at 100 °C, we obtained two ternary deep eutectic mixtures, *i.e.*, ChCl : Glc : H_2O (1 : 1 : 1) and (2 : 1 : 1), with significant differences in their physical and thermal properties (Table 1 and Fig. 1).

Both R-NADESs have high thermostability, starting to decompose at temperatures (T_{onset}) of 190 °C and 195 °C, respectively. Upon heating up to 105 °C, the equimolar ChCl : Glc : H_2O (1 : 1 : 1) R-NADES (entry 1, Table 1) loses less water than the ChCl : Glc : H_2O (2 : 1 : 1) R-NADES with higher molar content of choline chloride (entry 2, Table 1), which suggests a stronger binding of water in the hydrogen bond network of the equimolar deep eutectic mixture.

DSC analysis shows a significant difference between the melting behaviour of the choline chloride/glucose based ternary R-NADESs (Fig. 1A). The equimolar ChCl : Glc : H_2O (1 : 1 : 1) eutectic shows a clean thermogram, with only one peak at −44.5 °C, characteristic for the glass transition temperature (T_g), and without thermal transitions in the positive temperature range. However, the DSC trace of the ternary ChCl : Glc : H_2O (2 : 1 : 1) showed one distinct broad endothermic peak at 61.3 °C with onset at around 20 °C. Surprisingly, a small endothermic peak was observed at 73.6 °C, which can be ascribed to the excess ChCl not involved in the extended hydrogen bond network of the eutectic mixture. Aroso *et al.*,[33] observed similar peaks in the thermograms of mixtures of ChCl : xylose of 4 : 1 and 3 : 1, and concluded that the sharp endothermic peak at 78 °C of choline chloride resulting from a crystallographic arrangement phase transition, characteristic in the DSC of pure choline chloride, is shifted to lower temperatures, around 75 °C, in the DSC of mixtures, irrespective of the molar ratio and the composition of the eutectic mixture.

The viscosity of R-NADESs was measured between 40 and 80 °C, the optimum temperature range for a lipase-catalysed esterification reaction (Fig. 1B). Both eutectics were clear, colourless, and stable liquids in this temperature range. The viscosity decreased with increasing temperature following an Arrhenius-like behaviour; at higher temperatures the internal resistance of molecules decreases, and they flow more easily.

Table 1 Properties of R-NADES

	R-NADES		TGA		DSC		Viscosity (cP)		
Entry	Composition	Water content (%)	Weight loss at $T < 105$ °C (%)	T_{onset} (°C)	T_m (°C)	T_g (°C)	60 °C	70 °C	80 °C
1	ChCl : Glc : H_2O (1 : 1 : 1)	5.5	1.25	190	n. o.[a]	−44.5	1583	767.5	425
2	ChCl : Glc : H_2O (2 : 1 : 1)	3.8	2.86	195	61.3; 73.6	n. o.[a]	687	382	238

[a] n. o. – not observed.

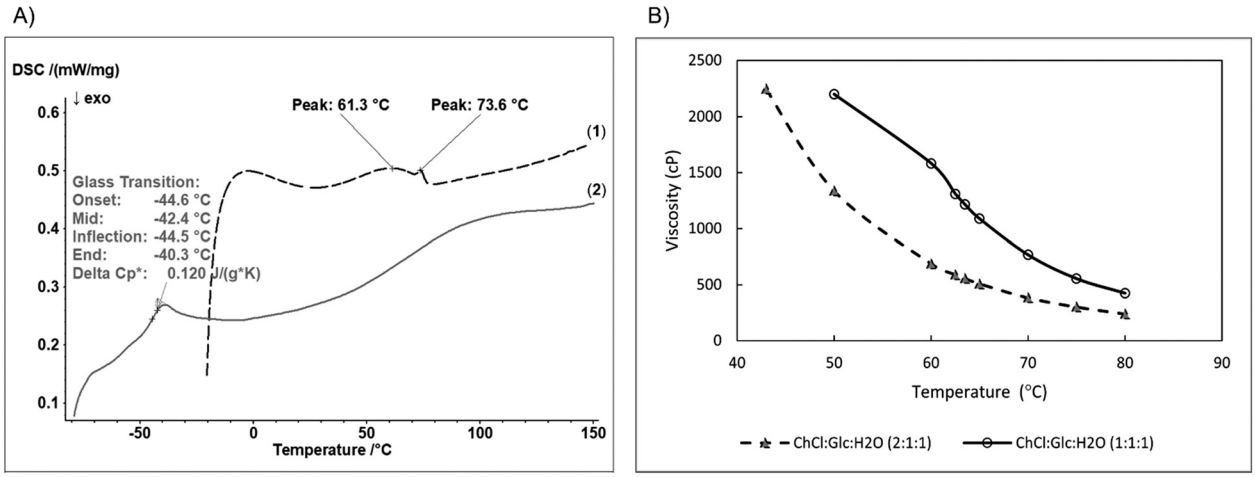

Fig. 1 (A) DSC thermograms and (B) viscosity of ChCl : Glc : H_2O (1 : 1 : 1) and (2 : 1 : 1) eutectic mixtures.

The decrease of viscosity with increasing temperature is spectacular. For example, an almost halving of the viscosity is obtained with every 10 °C increase of the temperature for both ternary choline chloride/glucose eutectic mixtures, as illustrated in Fig. 1B and Table 1. However, the viscosity of the ChCl : Glc : H_2O (1 : 1 : 1) R-NADES is at least double that of the choline chloride richer mixture, *i.e.*, ChCl : Glc : H_2O (2 : 1 : 1), making it a less suited solvent for the enzymatic reactions, due to possible mass transfer limitations.

Computational simulations of the R-NADES mixtures. Computational simulations were used to understand the molecular interactions between the components of the deep eutectic mixtures and their mobility. First, we evaluated the average number and the type of molecules surrounding each NADES component by contact frequency analysis (see the Experimental section for a more detailed description). The interactions between the different molecules in the equilibrated media may indicate how these components behave over time, which ultimately will give us information about the behaviour of choline and glucose in the esterification process.

The analysis of atomic contacts in Fig. 2a for the 2 : 1 : 1 choline chloride, water, and glucose solution shows that the choline quaternary ammonium group interacts preferentially with chloride, as expected because of the opposite charges, but also with all the oxygen atoms of glucose and water. Consequently, the interactions between glucose molecules and between glucose and water molecules occur with slightly lower probability than the statistical value. The probability values for the interaction between glucose or water and chloride anions are similar to the statistical values. Moreover, no meaningful differences are observed in the distribution of the interaction probabilities between alpha- and beta-glucose molecules (see Fig. S1†). Similar results are obtained for the 1 : 1 : 1 choline chloride, water, and glucose solution.

Next, we evaluated the average number of H-bonds per molecule type. Taking into consideration previous works[31,34,35] we also included the chloride anions as acceptors in the H-bond evaluation. The results for ChCl :

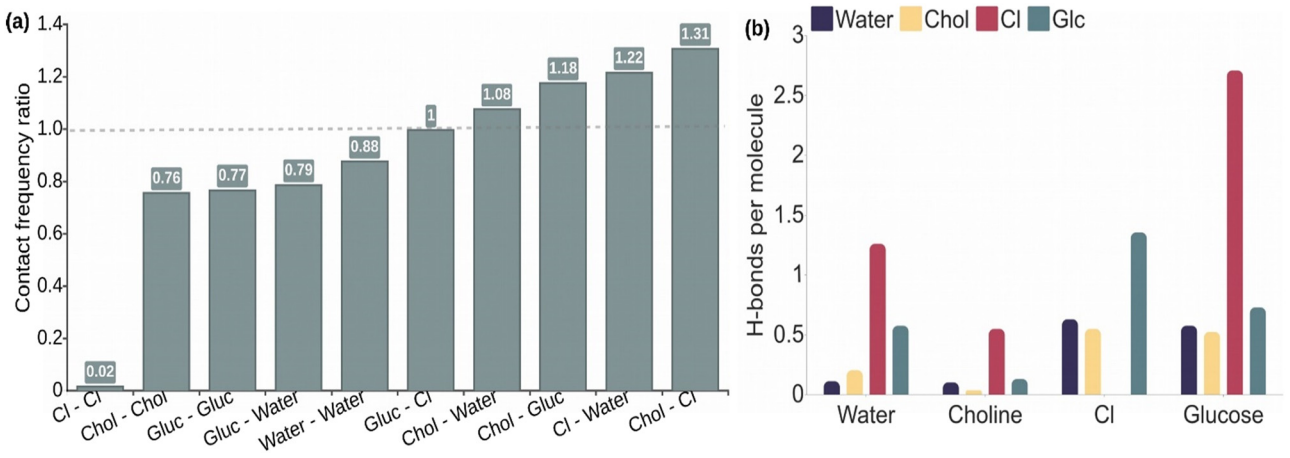

Fig. 2 Computational structural analysis of CalB in the glucose-based R-NADES (2 : 1 : 1). (a) Contact frequency ratio and (b) H-bond analysis between the different components in the R-NADES ChCl : Glc : H_2O (2 : 1 : 1) obtained from MD trajectories.

Glc : H_2O (2 : 1 : 1) in Fig. 2b show that the average number of H-bonds per molecule of glucose with chloride anions (2.7) is significantly higher than those evaluated with other molecules, with values lower than 1, including glucose–glucose H-bond interactions. The same trend occurs for water molecules, although the number of H-bonds per water molecule with chloride anions is lower, *i.e.* around 1. Choline molecules are also able to form H-bonds with their hydroxyl group. They also show the highest H-bond probability with the chloride anion, but the value (0.5) is lower than the one obtained for glucose or water. The H-bond analysis of alpha- and beta-glucose molecules in Fig. S2† shows, in general, similar probabilities per molecule. Nevertheless, it is noticeable that the H-bond probabilities between alpha and beta glucoses are slightly higher than between the same isomers.

The evaluation of the average number of H-bonds for each polar atom of glucose and choline molecules as shown in Fig. S3† shows a similar behaviour for all hydroxyl groups of glucose, while that for hemiacetal oxygen (O5) has significantly lower H-bond probabilities. We note that hemiacetal oxygen can only act as a H-bond acceptor in contrast with the dual role of donor or acceptor that can be adopted by the hydroxyl groups. As seen before, the hydroxyl groups preferentially form H-bonds with chloride anions with a probability per molecule of 0.5, while the interaction with other glucose molecules has a probability of 0.25–0.3. The number of H-bonds per glucose molecule with water and with choline is even lower, *i.e.* around 0.1. Noticeably, a similar distribution of probabilities is found for the hydroxyl group of the choline molecule with the difference that the probability of H-bond formation between choline molecules is the lowest. The results obtained in equimolar ChCl : Glc : H_2O (1 : 1 : 1) R-NADES are, in general, similar as those described here for the ChCl : Glc : H_2O (2 : 1 : 1) R-NADES, with the main difference showing higher values of glucose–glucose and choline–glucose H-bonds (see Fig. S4†).

Altogether, the simulations of glucose-based NADESs indicate the importance of the electrostatic interactions that lead to the organization of the components in the NADES to stabilize the ions of the mixture. Thus, besides the high interaction probability between choline and chloride ions, water and glucose molecules are preferably interacting with the charged molecules, taking advantage of their dual role as an electronic acceptor and donor. In agreement with previous works that carried out MD simulations of glucose in ionic DES,[31,34,35] the H-bond network formed in the NADES is mainly characterized by the interaction of the chloride anions with glucose. Although the participation of halide ions in H-bonds is not standard in biosystems, their study is well documented in the literature.[36] Indeed, the behaviour of halide ions as electron donors is different as the typical role of O atoms, since the negative charge of the first is delocalized allowing the simultaneous formation of many (6–7) H-bonds.[36] Each glucose molecule establishes an average of 2–3 H-bonds with chloride anions. Water molecules showed a similar behaviour, although the average number of H-bonds per water molecule with chloride is lower, around 1. It is noticeable that the participation of choline molecules in the H-bond network is significantly lower than the other NADES components, principally in the ChCl : Glc : H_2O (2 : 1 : 1) R-NADES.

Catalytic activity and thermal stability of LAR in glucose-based R-NADESs as a reaction medium

The esterification activity of the commercially available immobilized lipase B from *Candida antarctica* (LAR) was evaluated in the esterification of 1-propanol with LA, in both ChCl : Glc : H_2O (1 : 1 : 1) and (2 : 1 : 1) R-NADES mixtures, compared to the solvent free system as reference. LAR showed considerable esterification activity in R-NADESs, but is almost half compared to that in the solvent free system (Fig. 3A).

This significant decrease could be caused by the relatively high viscosity of the carbohydrate-based R-NADESs, which might slow down the diffusion and collision of reactant molecules with each other and with the enzyme. However, other effects of the medium on the enzyme cannot be excluded, as interactions between the eutectic mixtures and enzyme with either activating or inhibiting effects have been reported.[13]

Stability studies, conducted by preincubation of LAR at 70 °C in the R-NADES for 0, 24, 48 and 72 hours, followed by the determination of the esterification activity for *n*-propyl laurate synthesis, showed a remarkable high stability of LAR in the ChCl : Glc : H_2O (2 : 1 : 1) eutectic mixture, keeping more than 96% of the activity upon incubation for 72 hours at 70 °C (Fig. 3B).

These results suggest a stabilizing effect of the tertiary structure of the enzyme upon the interaction with the hydrophilic eutectic mixture and its constituents, and particularly with the polyhydroxy HBD, as also reported by Cao *et al.*[12]

Esterification reactions catalysed by LAR in the ChCl : Glc : H_2O (2 : 1 : 1) R-NADES

The synthetic experiments were focused on the selection of three parameters with a major impact on the conversion and product yield, namely enzyme load, temperature and mixing. The intervals for the variation of reaction parameters were selected based on the knowledge we acquired in our previous studies on lipase esterification reactions in choline chloride-carbohydrate polyol (1 : 1) R-NADES mixtures.[18] Small scale experiments carried out for 24 h at three temperatures, *i.e.*, (i) 60 °C and 30 rpm in a benchmark rotator, and (ii) at 70 °C and 75 °C in a thermomixer at 600 rpm, showed only minor differences between the LA conversions obtained (data not shown). This suggests that the better homogenisation of the eutectic mixture obtained by the combined rotation/oscillation mixing of the benchmark rotator partly

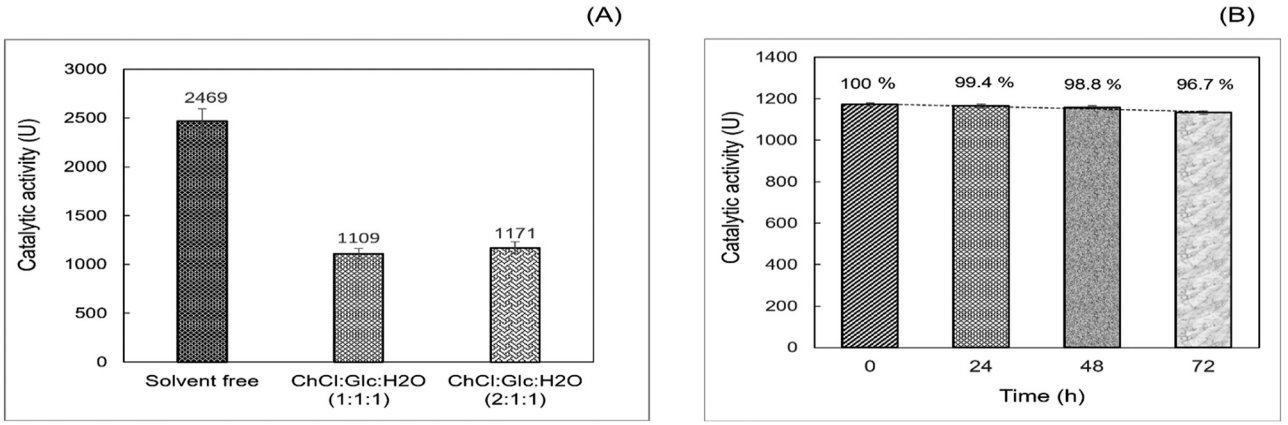

Fig. 3 (A) Catalytic activity (U) of LAR determined in the acylation of *n*-propanol with LA in the solvent free system at 55 °C, and in ChCl : Glc : H2O (1 : 1 : 1) and (2 : 1 : 1) R-NADESs, at 70 °C; (B) thermal stability of LAR in the ChCl : Glc : H2O (2 : 1 : 1) R-NADES, at 70 °C, assayed for the esterification of *n*-propanol with LA at 1 : 1 molar ratio.

compensates for the increase of temperature at a less efficient homogenisation in the thermomixer.

Enzyme load, though, significantly increased the LA conversion in the LAR-catalysed esterification of the ChCl : Glc : H_2O (2 : 1 : 1) NADES, as shown in Table 2. A 5-fold increase of LA conversion was observed upon increase for enzyme load from 800 U $g_{glucose}^{-1}$ to 1600 U $g_{glucose}^{-1}$. Minor LA conversions were obtained for reactions carried out in the equimolar ChCl : Glc : H_2O (1 : 1 : 1) NADES (not shown), the much higher viscosity probably impeding the reaction. Therefore, the next experiments were carried out only in the ChCl : Glc : H_2O (2 : 1 : 1) R-NADES.

Small scale preparative esterification reactions performed at the highest enzyme load in the ChCl : Glc : H_2O (2 : 1 : 1) R-NADES allowed the separation and characterisation of the reaction products. Progress of the reaction was monitored by HPLC, which showed a decreasing LA peak at R_t = 7.70 min, and an increasing peak at R_t = 9.54 min, which can be assigned to the reaction product (Fig. S6†). The reaction product was also visualised using TLC, where we observed an isolated spot with R_f = 0.73, next to LA, with R_f = 0.27 (Fig. S5†). The FTIR spectrum of the extract showed two sharp peaks at (a) 1737.8 cm^{-1} and (b) 1708.5 cm^{-1}, assigned to the –C═O vibrations of an ester (a) and a carboxylic acid (b), respectively (Fig. S7†). Chromatographic fractionation of the product mixture allowed the isolation of the ester product.

The formation of lauroylcholine chloride as the single esterification product was demonstrated by ^{1}H-NMR, where the characteristic signals for choline laurate were identified: ^{1}H-NMR $CDCl_3$, δ (ppm): 0.87 (t, 3H); 1.23–1.29 (m, 18H); 2.26–2.31 (t, 2H); 3.66 (s, 9H); 3.52 (t, 2H); 4.10 (t, 2H).

These spectral band assignments are in concordance with previously reported spectra for lauroylcholine chloride.[37]

Based on these results, we can conclude that in the lipase-catalysed esterification of the ChCl : Glc : H_2O (2 : 1 : 1) R-NADES, the reaction product is the lauryl ester of choline chloride (see Scheme 2), and not the glucose ester. We assume that only the not-charged choline chloride that is not tightly bound with glucose and water in the extended hydrogen bond network can enter the alcohol catalytic subsite of the enzyme and is transformed.

Table 2 Effect of enzyme load on the LA conversion during the esterification of the ChCl : Glc : H_2O (2 : 1 : 1) R-NADES at 60 °C and 72 h incubation

Code	Enzyme load (U $g_{glucose}^{-1}$)	LA conversion (mol%)
Control	—	—
R1	800	10
R2	1200	30
R3	1600	53

Molecular modelling and simulations

Molecular modelling and simulations of the motion of the molecules composing the R-NADES-hydrogen bond network in the presence of the biocatalyst and of lauric acid, the co-substrate for ester synthesis, were applied to get insight into the mechanism of this reaction.

Simulations of the ChCl : Glc : H_2O (2 : 1 : 1) NADES including CalB and lauric acid. As in our previous work,[18] the MD simulations including CalB lipase and lauric acid showed the separation of the mixture in two phases, one formed by lauric acid and the other by the R-NADES, locating the protein at the interface. Likewise, the CalB catalytic site faces the acyl phase as described by the experiments.[38] Our simulations show that no molecules of glucose or choline travel from the R-NADES phase to the acyl phase. On the contrary, water molecules were found entering the acyl phase with a rate of around 4–5 water molecules every 10 ns (in a surface of approx. 10 × 10 nm). Moreover, stable interactions between several molecules of glucose and choline and the CalB surface residues are present along our trajectories, including those protein surface sites in contact with the acyl phase.

Regarding the catalytic pocket, different lauric acid molecules enter in the catalytic pocket along the trajectories,

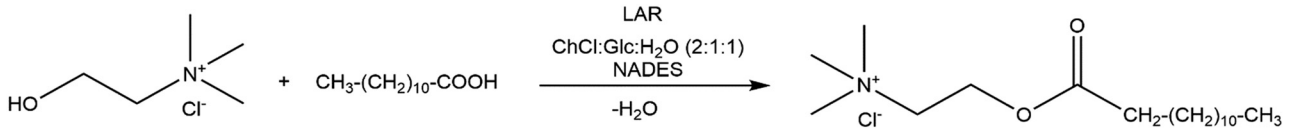

Scheme 2 Synthesis of lauroylcholine chloride by immobilised CalB (LAR) in the ChCl : Glc : H_2O (2 : 1 : 1) R-NADES.

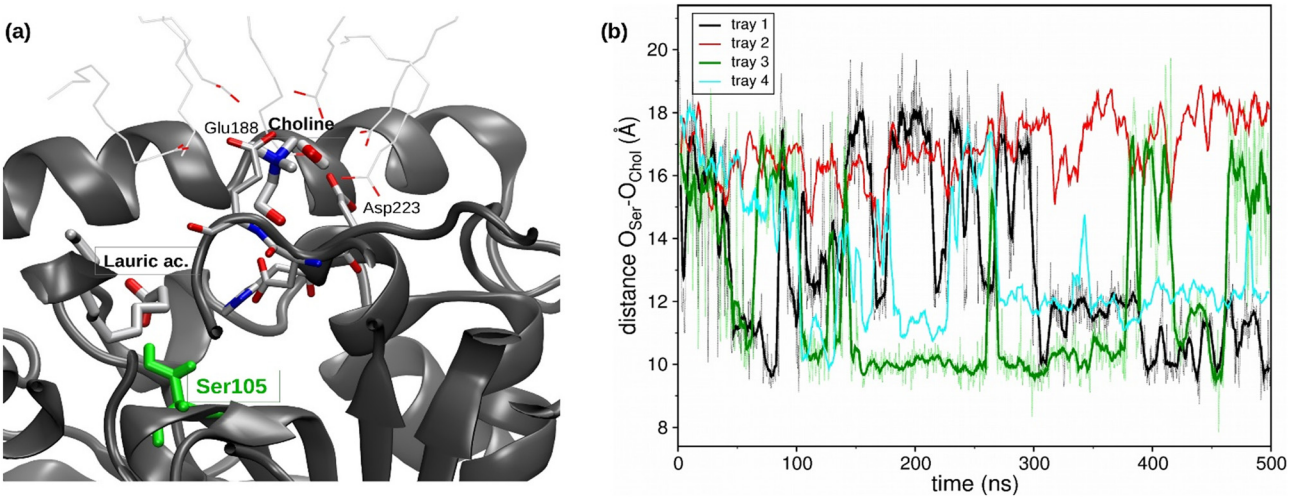

Fig. 4 Computational structural analysis of CalB in the glucose-based NADES (2 : 1 : 1). (a) Representative snapshot of the CalB catalytic pocket from MD trajectories of CalB in ChCl : Glc : H_2O : LA (2 : 1 : 1 : 1), in which the binding between a lauric acid molecule and Ser105 and the location of a choline molecule interacting with Glu188 and Asp223 occur. (b) Evolution of the atomic distance between the hydroxyl oxygens of Ser105 and the choline molecule at the entrance of the pocket in the same MD trajectories.

and the formation of the H-bond between the carboxy group of a lauric acid and the hydroxyl group of the catalytic residue Ser105 can be observed (see Fig. 4a), which precedes the esterification reaction.

Moreover, a choline molecule is found at the entrance of the pocket. The cation is stabilized in this location, inside the acyl phase at the protein surface, by the electrostatic interaction with the residues Glu188 and Asp223, as well as by different water molecules and carboxylic groups of the lauric acid molecules (see Fig. 4a). The distance between the oxygen of the Ser105 hydroxylic group and the oxygen of the hydroxyl group of choline was evaluated along the MD trajectories (see Fig. 4b). The entrance of choline in the pocket could not be observed within the simulation time (4 runs of 500 ns), which may indicate that this event is a bottleneck of the esterification reaction. However, the hydroxyl group of choline was correctly oriented towards the pocket inside in different stages of the trajectories, which coincides with the shortest Ser105-choline distances of around 8–10 Å. These observations were also found in the simulations of the ChCl : Glc : H_2O (1 : 1 : 1) R-NADES (see Fig. S5†). However, the measured distances between Ser105 and choline were higher, and a stable conformation at 8–10 Å distance, as in ChCl : Glc : H_2O (2 : 1 : 1) R-NADES, was not found.

Simulations without lauric acid. Additional MD simulations of the R-NADES with the CalB protein were performed to evaluate the interactions of the R-NADES components in the catalytic site at the extreme scenario of infinite dilution of lauric acid. Without the acyl phase, choline and glucose molecules would have the highest chances of reaching the entrance of the catalytic pocket. In a similar way to what was observed in our previous work of CalB in a polyol-based R-NADES,[18] the pocket size of the protein is smaller when it is dissolved in the R-NADES without the presence of the acyl phase. In this scenario, the entrance of water molecules inside the pocket is the most frequent phenomenon observed in our simulations. Nevertheless, the entrance of glucose molecules has been observed, but always through the acyl subsite, which shows a broader space along the trajectories. A careful analysis of the contacts of the glucose molecule during the entrance event shows us that it still conserves the interactions with chloride ions and other components of the bulk, which accompany glucose during this stage (see Fig. 5a). On the other hand, a choline molecule is at the same location that it was found in simulations with lauric acid, *i.e.* at the entrance of the pocket interacting with the residues Glu188 and Asp223. The partial entrance of choline molecule in the alcohol subsite now occurs in one of our trajectories, achieving a distance to Ser105 of 6.64 Å (see Fig. 5b).

Discussion. Overall, simulations of R-NADES + CalB + LA showed the impermeability of the acyl phase, towards which the CalB catalytic site is faced, for the glucose and choline molecules. This behaviour may be a consequence of the glucose-based R-NADES properties, as glucose hydroxyl groups participate in the stabilization of the charged

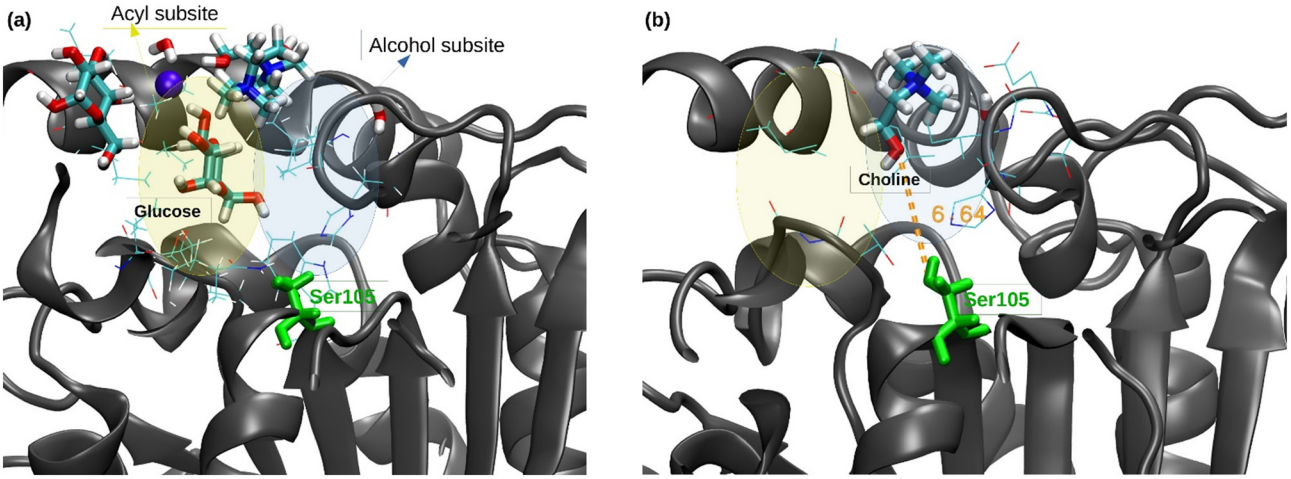

Fig. 5 Graphical representation of (a) the entrance event of glucose and (b) the particle entrance of choline in the catalytic pocket obtained from the MD trajectories of CalB in the R-NADES ChCl : Glc : H2O (2 : 1 : 1).

molecules ChCl *via* electrostatic and H-bond interactions. The diffusion of glucose and choline molecules from the NADES bulk to the pocket entrance is a rare event. However, a stable binding of a choline molecule with the surface residues Glu188 and Asp223 located near the alcohol subsite of the catalytic pocket can be found in our simulations. Although the pocket entrance event of the choline molecule does not occur, the binding conformation of the choline is modified along the trajectory to orient the hydroxyl group towards the pocket inside at a distance to the catalytic residue Ser105 of 8 Å. In the MD trajectories without lauric acid, the partial entrance of a choline molecule in the alcohol subsite occurs, as the distance between the hydroxyl groups of Ser105 and choline decreases until 6.64 Å. On the other hand, the undesired entrance of a glucose molecule in the acyl subsite is observed in the same simulations. This behaviour may be caused by the role of the glucose molecules in the NADES. As they are interacting with a high number of chloride ions, the entrance in the catalytic pocket might be only possible in the acyl subsite, which has a bigger size in our simulations. The simulations lead to the conclusion that ternary equimolar choline chloride–glucose–water deep eutectic mixtures cannot function as reactive-NADESs with a dual role, as solvent and source of substrate, for the synthesis of lauryl glucose esters, due to the multiple and strong interactions in the H-bond network.

Nevertheless, when one of the R-NADES components is in excess, as in the case of the ChCl : Glc : H_2O (2 : 1 : 1) R-NADES, the free, not-bound choline chloride, is converted to the corresponding lauryl ester in the lipase-catalysed esterification reaction, as confirmed experimentally, and the eutectic mixture behaves as a reactive NADES.

Conclusions

In this study, we obtained and characterised two hydrophilic ternary choline chloride/glucose/water R-NADES mixtures, one with equimolar amounts of all three components, *i.e.*, ChCl : Glc : H_2O (1 : 1 : 1) and the second with a molar excess of choline chloride, *i.e.*, ChCl : Glc : H_2O (2 : 1 : 1). Computational simulations showed that both NADES mixtures consist of an extended network created by a high number of hydrogen bonds and electrostatic interactions. Both eutectic mixtures were fluids with low viscosity appropriate for biocatalysis at temperatures between 40 °C to 80 °C. Indeed, the immobilized *Candida antarctica* lipase B (LAR) showed substantial esterification activity and very high thermal stability in the two NADES systems, and this was all explained by computational simulations that showed stable interactions between several molecules of glucose and choline and the CalB surface residues in contact with the acyl phase. Moreover, simulations of the R-NADES-CalB-lauric acid system showed that the diffusion of glucose and choline molecules from the R-NADES bulk to the entrance of the catalytic pocket is rare. Although choline can enter the alcohol subsite in the right orientation of the alcohol group towards the catalytic Ser105, a stable binding of a choline molecule with the negatively charged Glu188 and Asp223 surface residues located near the alcohol subsite of the catalytic pocket might prevent choline esterification. Also, glucose molecules, which are associated with a high number of chloride ions by H-bonds, enter erroneously in the acyl subsite, with a similar effect of hindering esterification. Therefore, the ternary NADES mixtures examined do not show the double function as solvent and source of substrate. Indeed, this was confirmed experimentally for the equimolar ChCl : Glc : H_2O (1 : 1 : 1) R-NADES, when neither glucose nor choline chloride esters were produced upon reaction with lauric acid and immobilized CalB. Yet, lipase esterification of the rich choline chloride NADES ChCl : Glc : H_2O (2 : 1 : 1) did convert the unbound choline chloride, with compensated charge through the electrostatic interactions between the quaternary ammonium and the chloride ions, into the corresponding lauryl ester. In this case, the ChCl : Glc : H_2O

(2 : 1 : 1) does behave as a reactive R-NADES, being simultaneously the reaction medium and the substrate resource.

Lauroylcholine chloride is a valuable surfactant with applications in life sciences, health, pharmaceuticals, and cosmetics.[39,40] The method described in this paper might open the way for greener synthetic routes for this compound and for a wider range of choline chloride esters of medium and longer alkyl chain carboxylic acids.

Concluding on these results, we presume that fine tuning of the composition of ternary R-NADES mixtures towards an excess of one of the reactive substrates, *i.e.* choline chloride or glucose, will result in high yields of the selected esters. This will prevent synthetic challenges triggered by (lack of) solubility of substrates and interactions with the R-NADES components, which might affect reactivity. We believe that this approach can be applied to a large variety of natural deep eutectic mixtures, allowing the development of simpler processes with fewer steps. R-NADESs are not common solvents, which fit all solutions in the same way, and they need insightful studies for each case, considering substrate and enzyme compatibility.

Moreover, this work shows the constructive interaction between the experimental research and computation simulations in understanding the complex connections between enzymes, substrates, and the reaction medium, in this case the R-NADES, as well as how important it is to integrate them.

Data availability

The data supporting this article have been included as part of the ESI.†

Author contributions

Alina Ramona Buzatu (methodology, investigation, formal analysis, validation, writing – original draft preparation, writing – review and editing), Ioan Bîtcan (investigation and formal analysis), Diana Maria Dreavă investigation, formal analysis, and validation), Miguel Angel Soler (methodology, validation, investigation, supervision, writing – original draft preparation, writing – review and editing), Sara Fortuna (investigation and writing – original draft preparation), Ozge Ozkilinc (investigation, formal analysis, and writing – original draft preparation), Paolo Giannozzi (funding acquisition, writing – review and editing), Federico Fogolari (methodology, investigation, writing – review and editing, supervision, and funding acquisition), Lucia Gardossi (funding acquisition, writing – review and editing), Francisc Peter (funding acquisition, methodology, project administration, supervision, writing – review and editing), Anamaria Todea (conceptualization, validation, formal analysis, writing – original draft preparation, writing – review and editing), Carmen Gabriela Boeriu (conceptualization, methodology, funding acquisition, project administration, resources, supervision, validation, writing – original version preparation, writing – review and editing). All authors have read and agreed to the published version of the manuscript.

Conflicts of interest

There are no conflicts to declare.

Acknowledgements

This work was supported by a grant from the Romanian Ministry of Education and Research, CCCDI-UEFISCDI, project number PN-III-P4-ID-PCE-2020-2177, within PNCDI III, contract number PCE 157/2021. M. S. and O. O. are supported by the Italian Ministry of the University and the Research *via* the research program PON 2014-2020 AZIONE IV.6 GREEN, project numbers 2021RTDA46_02B2_DMIF and DOT215B2RJ, respectively. Financial support is acknowledged from ICSC – Centro Nazionale di Ricerca in High Performance Computing, Big Data and Quantum Computing, funded by European Commission – NextGenerationEU – PNRR, Missione 4 Componente 2 Investimento 1.4 Grant number CN00000013. The authors would like to thank Linda Gootjes for assistance with NMR measurements.

Notes and references

1 M. Verboni, D. R. Perinelli, A. Buono, R. Campana, M. Sisti, A. Duranti and S. Lucarini, *Antibiotics*, 2023, **12**, 1–9.
2 A. Paiva, R. Craveiro, I. Aroso, M. Martins, R. L. Reis and A. R. C. Duarte, *ACS Sustainable Chem. Eng.*, 2014, **2**, 1063–1071.
3 J. N. Tan and Y. Dou, *Appl. Microbiol. Biotechnol.*, 2020, **104**, 1481–1496.
4 T. Kobayashi, *Biotechnol. Lett.*, 2011, **33**, 1911–1919.
5 R. Croitoru, F. Fiţigău, L. A. M. Van Den Broek, a. E. Frissen, C. M. Davidescu, C. G. Boeriu and F. Peter, *Process Biochem.*, 2012, **47**, 1894–1902.
6 E. Zago, N. Joly, L. Chaveriat, V. Lequart and P. Martin, *Biotechnol. Rep.*, 2021, **30**, e00631.
7 L. A. M. Van Den Broek and C. G. Boeriu, *Carbohydr. Polym.*, 2013, **93**, 65–72.
8 H. Wang, Y. Tao, M. Vimbai, J. Cao, J. Yang, K. Huang, Y. Ge, Y. Yu, Z. Xiao, Y. Kuang, J. Huang and S. Yang, *J. Mol. Liq.*, 2023, **377**, 121379.
9 Á. Hernández, A. Vanessa, P. García, J. López, M. Luis, C. Caero, J. Trapala, C. Montiel, I. Bustos and J. Miquel, *J. Polym. Res.*, 2023, **30**, 1–6.
10 R. A. Sheldon and J. M. Woodley, *Chem. Rev.*, 2018, **118**, 801–838.
11 J. Cao, R. Wu, F. Zhu, Q. Dong and E. Su, *Biochem. Eng. J.*, 2022, **179**, 108336.
12 J. Cao, R. Wu, F. Zhu, Q. Dong and E. Su, *Enzyme Microb. Technol.*, 2022, **157**, 110022.
13 R. Hollenbach, K. Ochsenreither and C. Syldatk, *Int. J. Mol. Sci.*, 2020, **21**, 1–11.

14 M. Pöhnlein, J. Ulrich, F. Kirschhöfer, M. Nusser, C. Muhle-Goll, B. Kannengiesser, G. Brenner-Weiß, B. Luy, A. Liese, C. Syldatk and R. Hausmann, *Eur. J. Lipid Sci. Technol.*, 2015, **117**, 161–166.
15 R. Semproli, S. N. Chanquia, J. P. Bittner, S. Müller, P. Domínguez de María, S. Kara and D. Ubiali, *ACS Sustainable Chem. Eng.*, 2023, **11**, 5926–5936.
16 R. Hollenbach, B. Bindereif, U. S. van der Schaaf, K. Ochsenreither and C. Syldatk, *Front. Bioeng. Biotechnol.*, 2020, **8**, 1–10.
17 S. Siebenhaller, T. Hajek, C. Muhle-Goll, M. Himmelsbach, B. Luy, F. Kirschhöfer, G. Brenner-Weiß, T. Hahn, S. Zibek and C. Syldatk, *Bioresour. Bioprocess.*, 2017, **4**, 1–9.
18 A. R. Buzatu, M. A. Soler, S. Fortuna, O. Ozkilinc, D. M. Dreavă, I. Bîtcan, V. Badea, P. Giannozzi, F. Fogolari, L. Gardossi, F. Peter, A. Todea and C. G. Boeriu, *Catal. Today*, 2024, **426**, 1–18.
19 L. Martínez, R. Andrade, E. G. Birgin and J. M. Martínez, *J. Comput. Chem.*, 2009, **30**, 2157–2164.
20 J. Uppenberg, M. T. Hansen, S. Patkar and T. A. Jones, *Structure*, 1994, **2**, 293–308.
21 S. Jo, T. Kim, V. G. Iyer and W. Im, *J. Comput. Chem.*, 2008, **29**, 1859–1865.
22 P. Bauer, B. Hess and E. Lindahl, *GROMACS 2022 Source code*, 2022.
23 J. Huang, S. Rauscher, G. Nawrocki, T. Ran, M. Feig, B. L. De Groot, H. Grubmüller and A. D. MacKerell, *Nat. Methods*, 2016, **14**, 71–73.
24 E. R. Hatcher, O. Guvench and A. D. MacKerell, *J. Chem. Theory Comput.*, 2009, **5**, 1315–1327.
25 J. B. Klauda, R. M. Venable, J. A. Freites, J. W. O'Connor, D. J. Tobias, C. Mondragon-Ramirez, I. Vorobyov, A. D. MacKerell and R. W. Pastor, *J. Phys. Chem. B*, 2010, **114**, 7830–7843.
26 J. P. Bittner, L. Huang, N. Zhang, S. Kara and S. Jakobtorweihen, *J. Chem. Theory Comput.*, 2021, **17**, 5322–5341.
27 B. Hess, H. Bekker, H. J. C. Berendsen and J. G. E. M. Fraaije, *J. Comput. Chem.*, 1997, **18**, 1463–1472.
28 G. Bussi, D. Donadio and M. Parrinello, *J. Chem. Phys.*, 2007, **126**, 014101.
29 M. Parrinello and A. Rahman, *J. Appl. Phys.*, 1981, **52**, 7182–7190.
30 M. Berrera, H. Molinari and F. Fogolari, *BMC Bioinf.*, 2003, **26**, 1–26.
31 Z. Sailau, N. Almas, A. Aldongarov and K. Toshtay, *J. Mol. Model.*, 2022, **28**, 1–8.
32 W. Humphrey, A. Dalke and K. Schulten, *J. Mol. Graphics*, 1996, **14**, 33–38.
33 I. M. Aroso, A. Paiva, R. L. Reis and A. R. C. Duarte, *J. Mol. Liq.*, 2017, **241**, 654–661.
34 M. Mohan, P. K. Naik, T. Banerjee, V. V. Goud and S. Paul, *Fluid Phase Equilib.*, 2017, **448**, 168–177.
35 S. Barani Pour, J. Jahanbin Sardroodi and A. Rastkar Ebrahimzadeh, *J. Mol. Liq.*, 2021, **334**, 115956.
36 I. Pethes, I. Bakó and L. Pusztai, *Phys. Chem. Chem. Phys.*, 2020, **22**, 11038–11044.
37 **https://spectrabase.com/compound/F4mxjBjVUeC**.
38 C. C. Gruber and J. Pleiss, *J. Mol. Catal. B: Enzym.*, 2012, **84**, 48–54.
39 A. Tolentino, A. Alla, A. Martínez De Ilarduya, M. Font-Bardía, S. León and S. Muñoz-Guerra, *RSC Adv.*, 2014, **4**, 10738–10750.
40 R. Angius, S. Murgia, D. Berti, P. Baglioni and M. Monduzzi, *J. Phys.: Condens. Matter*, 2006, **18**, S2203–S2220.